THE AMERICAN SOCIETY OF MECHANICAL ENGINEERS
345 E. 47th St., New York, N.Y. 10017

94-GT-219

WAKE-INDUCED UNSTEADY FLOWS: THEIR IMPACT ON ROTOR PERFORMANCE AND WAKE RECTIFICATION

J. J. Adamczyk
NASA Lewis Research Center
Brook Park, Ohio

M. L. Celestina
Department of Aeromechanics
Sverdrup Technology, Inc.
Brook Park, Ohio

Jen Ping Chen
NSF Engineering Research Center
Mississippi State University
Mississippi State, Mississippi

ABSTRACT

The impact of wake–induced unsteady flows on blade row performance and the wake rectification process is examined by means of numerical simulation. The passage of a stator wake through a downstream rotor is first simulated using a three dimensional unsteady viscous flow code. The results from this simulation are used to define two steady state inlet conditions for a three dimensional viscous flow simulation of a rotor operating in isolation. The results obtained from these numerical simulations are then compared to those obtained from the unsteady simulation both to quantify the impact of the wake–induced unsteady flow field on rotor performance and to identify the flow processes which impact wake rectification. Finally, the results from this comparison study are related to an existing model which attempts to account for the impact of wake–induced unsteady flows on the performance of multistage turbomachinery.

INTRODUCTION

Turbomachinery is able either to impart or to remove energy from a flow stream because the flow within is inherently unsteady. This simple fact is overlooked by many researchers for this reason: when analyzing the flow through an isolated rotating blade row the dependence on time may be eliminated by transforming to a coordinate system fixed to the blade row. However, as soon as one attempts to address the flow through more than one blade row, the role of time becomes self–evident. As an example, time appears explicitly in the form of a local time derivative of pressure in the equation governing the time rate of change of the total enthalpy of a fluid particle. For multi–blade row configurations this term can not be removed by a trivial transformation of coordinates.

A procedure for grouping, according to flow processes, the unsteady terms which impact the performance of blade rows within single and multistage turbomachinery was developed by Adamczyk (1984). This grouping procedure was based on the closure terms which account for the presence of neighboring blade rows in his average–passage equation system. These equations govern the time–average flow field of a typical passage of a blade row. Within this equation system, the surrounding blade rows make their presence known through a system of body forces, a number of energy sources or sinks, a set of velocity correlations similar in form to the Reynolds stresses, and a correlation involving both the unsteady total enthalpy field and the unsteady velocity field. These terms serve as 'mail boxes' in which to place (and hence group) the various unsteady flow processes occurring within multi–blade row turbomachinery.

In this paper, the topic of wake–induced unsteady flows as it affects the performance of a rotor of an axial flow compressor will be addressed. Specifically, the need to account for the wake–induced unsteady flows set up by an upstream stator in predicting rotor performance will be examined. In addition, the related topic of wake rectification will also be addressed. The various flow processes associated with the unsteady processes will be related to the closure terms in the average–passage equation system. The study will be undertaken using the results from a series of numerical simulations.

Atkins and Smith (1982) argued that mixing brought about by secondary flows had a significant impact on the radial distribution of the axisymmetric flow properties in multistage axial flow compressors. Included in the definition of the secondary flow field was the effect of the wakes. In the Atkins and Smith (1982) model, the mixing within a blade row is the result of a superpositioning of the secondary flow generated by the blade row itself plus that generated by all the blade rows upstream. The major contributor to this mixing process was the secondary flow set up by the blade row immediately upstream. Hence, the mixing process Atkins and Smith (1982) are modeling is unsteady and comes about by the interaction between the incoming unsteady secondary flow field and the downstream blade row.

The first publication on the topic of wake rectification as a result of circumferential mixing was that of Kerrebrock and

Presented at the International Gas Turbine and Aeroengine Congress and Exposition
The Hague, Netherlands — June 13–16, 1994
This paper has been accepted for publication in the Transactions of the ASME
Discussion of it will be accepted at ASME Headquarters until September 30, 1994

Mikolajczak (1970). They showed that wakes from a rotor are rectified as they pass through a downstream stator yielding an increase in total temperature on the pressure surface of the stator, which is another form of wake blade row interaction. This work has been used by compressor aerodynamicists as a diagnostic tool for estimating the performance of a rotor. Kerrebrock and Mikolajczak (1970) used the results of their analysis to infer the performance of a rotor from measurements taken downstream of a stator. However, they make no attempt to relate their findings to the performance of the stator. Very recently their analysis has been used by Butler et al. (1989) as well as others in the study of thermal loads generated by hot streaks in turbines.

We begin the present study by addressing the importance of including the effects of wake–induced unsteady flows in the description of the time–averaged flow field across a rotor operating downstream of a stator. If no significant reason can be given for including these effects, then one may seriously question their impact on the inter rotor blade row flow field. This part of the present work is intended to demonstrate at the very minimum the need to include the radial mixing process described by Atkins and Smith (1982) in the modeling of the time–averaged three dimensional flow field within a typical passage of a blade row embedded within a multistage configuration. This study will be followed by an analysis of the stator wake rectification.

The stator configuration used in this study has a corner separation at the junction of the hub and the suction surface. This separation leads to a very thick wake which is acted upon by the lower portion of the downstream rotor. The thick wake helps to accentuate the effects of the unsteady deterministic flow field associated with the wake on the rotor performance. The numerical codes used in this study are three dimensional, compressible and viscous, with the effects of turbulence introduced through the model proposed by Baldwin and Lomax (1978). The shear force acting on solid surfaces is modeled using wall functions. In addition, these surfaces are assumed to be adiabatic. One of the codes solves for the time–averaged flow field surrounding a blade row embedded in a multistage configuration and has been reported upon by Adamczyk et al. (1990). The other is a recently developed time–dependent code which simulates the passage of a wake through a blade row and is reported upon by Chen et al. (1993). This unsteady code uses an implicit integration scheme to advance the solution in time and is second order accurate in both space and time. Using the results from a temporal accuracy study reported in Chen et al., a time step of one–fourth of a wake passing cycle was used in the unsteady simulation. In all the simulations, a common grid was used consisting of 31 radial points, 31 circumferential points, and 31 points distributed along the chord of each blade row. Based on previous simulations of similar configurations, this grid density was deemed adequate for the purpose of this study. However, this grid density requires the use of wall functions to establish the shear force acting on solid surfaces.

PERFORMANCE OF AN EMBEDDED BLADE ROW

The impact of the unsteady flow field generated by a blade row on the performance of a downstream blade row is investigated through numerical experimentation. As stated earlier, the geometry is that of a compressor stage consisting of a stator followed by a rotor. These blade rows are subsonic and are representative of embedded blade rows within a multistage axial flow compressor. The first simulation executed used the average–passage code. The output from this simulation was used to define the inlet conditions in an unsteady simulation of the rotor flow field. By comparing the results of this time–dependent simulation to that in which the rotor is modeled as an isolated blade row, the effects of the unsteady deterministic flow field on the rotor's performance can be quantified. This exercise could have been undertaken using the average–passage code if the value of the closure terms as modeled in this code were identical to those derived from the unsteady simulation. However, because the physics associated with wake cutting and intra–blade row transport is not accounted for in the current closure model, any conclusions drawn from the results of the average–passage code could be questioned. From the rotor unsteady flow simulation the axial, absolute tangential, and radial velocity components, as well as the absolute total temperature and pressure were averaged over time and circumference to define the radial distribution of the time–averaged yaw and pitch angle, in addition to the absolute total temperature and pressure of the flow entering the rotor. These flow quantities were further averaged over span and used to establish the corrected flow to the rotor. In this work, these averaged flow quantities are used to define the inlet conditions to the rotor as if it were operating in isolation. The grid for this simulation is identical to that used in the unsteady flow simulation. Figure 1 shows the radial distribution of the circumferential average of the product of density and axial velocity, density and absolute tangential velocity, and density and radial velocity from the isolated rotor simulation compared to that derived from the unsteady simulation at the common inlet plane. Also presented are the resulting inlet total pressure distributions. Because the two inlet total temperature distributions are identical, both being uniform across the span and equal to the total temperature at the stator inlet, they are not presented. As can be seen in the figure, the inlet conditions for the isolated rotor simulation very nearly match those derived from the unsteady simulation. Note that all the flow variables in this figure and in all subsequent figures are normalized with respect to the total conditions upstream of the stator.

Figure 1 also includes a plot of the radial distribution of the circumferential average of the pressure from the unsteady and isolated rotor simulation at the common inlet plane. The unsteady distribution is also averaged over time. Note the difference between the two curves, which at the hub amounts to 20% of the inlet flow dynamic head. This difference, which is not negligible, is related to the magnitude of the time variation of the inlet dynamic head. This term is equal to one half the sum of the diagonal elements of the temporal velocity correlation tensor.

Figure 2 shows plots of the mass–averaged radial distribution of the absolute total temperature and pressure at the common exit plane for both simulations. The unsteady simulation results are also mass–averaged over time. Since the inlet absolute total temperature specified in the isolated rotor simulation is identical to its unsteady counterpart, the differences seen are once again the result of an unsteady incoming flow field to the rotor. The

absolute total temperature curves show the energy input to the flow to be larger in the case of the isolated rotor. The total pressure plots show a similar behavior. The last plot of this figure shows the efficiency as derived from the simulation of the isolated rotor and the unsteady case. The efficiency is evaluated from the respective inlet and exit mass–averaged total pressure and temperature distributions. In the hub region, the efficiency of the isolated rotor is far greater than that of the rotor operating downstream of the stator. Outboard of thirty–five percent of span, the efficiency of the isolated rotor is less than that of the rotor downstream of the stator. The differences in the hub region result from there being far more radial and circumferential movement of fluid particles in the unsteady simulation than is occurring in the isolated rotor simulation. The reversal between the two efficiency plots outboard of thirty–five percent of span is associated with the unsteady interaction between the incoming stator wake and the pressure field. This interaction will be discussed in the section dealing with wake rectification.

Based on the work of Stewart (1959), Dring and Spear (1991) and also Dawes (1992) suggested that a blade row within a multistage machine could be modeled as an isolated blade row provided that the inlet conditions were those derived from passing the unsteady flow exiting the upstream blade row through a mixing plane. Across this mixing plane the mass flux, axial impulse, flux in tangential and radial momentum, and flux in total enthalpy are conserved. This mixing plane model assumes that there is little if any impact of the unsteady intra–blade row flow processes on performance. Hence this model is unable to account for the mixing process outlined by Atkins and Smith (1982). Following the work of Dring and Spear (1991), the output from the average–passage simulation of the stator was used in conjunction with a mixing plane analysis to extract the required inlet conditions for simulating the downstream rotor. The results of this analysis are presented in a format identical to that used for figures 1 and 2. Figure 3 shows plots of the radial distribution of the product of axial velocity and density, absolute tangential velocity and density, radial velocity and density, absolute total pressure and pressure at the inlet plane. To generate these plots, the results from the mixing plane model were averaged over the circumferential direction. In the case of the unsteady results, they were also averaged over time. The corrected weight flow per unit area upstream of the mixing plane matches that of the rotor in the unsteady simulation.

Figure 3 shows that a significant difference exists between the profiles of tangential and radial velocity as derived from the mixing plane model and their respective counterparts derived from the unsteady simulation. This difference is a direct measure of the magnitude of the temporal correlation involving the product of the axial and tangential velocities in the one case and the product of the axial and radial velocities in the other. These correlations account for the transport of axial momentum in the tangential and radial directions associated with the unsteady flow entering the rotor. The differences in the magnitude of the velocity components also imply differences in the yaw and pitch angle of the fluid entering the rotor. The two curves of absolute total pressure show that the mixing model yields values which are "higher" than those derived from the unsteady simulation. This result is unexpected, for one would argue that in an irreversible mixing process there should be a loss in total pressure rather than a gain. This odd result is easily explained by noting that what is being plotted in the case of the unsteady simulation is the time–averaged total pressure entering the rotor as opposed to its mass–averaged value as is needed to estimate the loss due to mixing. Had the mass–averaged total pressure distribution associated with the unsteady simulation been plotted, one would indeed see that there was a loss in total pressure as a result of the modeled mixing process. We chose not to present the mass–weighted total pressure curve associated with the unsteady simulation to dramatize the fact that the unsteady flow is not mixed out prior to entering the rotor and thus the wake mixing is taking place within the rotor passage under conditions which are not accounted for by the mixing plane model. Finally, note that the inlet plane pressure distributions are also different and that, as previously stated, this difference is caused by the unsteady flow generated by the stator.

Figure 4 shows plots of the absolute total temperature and pressure, mass–averaged circumferentially, as a function of span at the exit plane. The results from the unsteady rotor simulation (as in Figure 2) were also mass–averaged over time. Since the total temperature of the flow stream entering the rotor is identical for both cases, the total temperature plot also indicates the energy input to the flow stream by the rotor. It appears that the rotor operating downstream of the mixing plane is putting more energy into the flow than it would in the unsteady flow environment. The total pressure plots show a similar behavior. The difference between the results from the unsteady simulation and those from the mixing plane model increases with distance from the hub. This difference between the two sets of results appears to be caused by the larger radial movement of fluid particles in the unsteady simulation.

The last plot of Figure 4 shows the efficiency derived from total pressure and temperature distributions aft and forward of the mixing plane. For comparison purposes the efficiency as derived from the unsteady rotor simulation is also shown and is identical to that presented in Figure 2. The efficiency as derived from the flow condition downstream of the mixing plane is greater than that derived from the unsteady simulation over most of the span. This difference occurs because no account has been taken of the loss in total pressure across the mixing plane. If one uses the flow conditions upstream of the mixing plane to establish the efficiency of the rotor, the agreement between that derived from the unsteady simulation and that from the mixing plane simulation is considerably improved. However, by doing so we raise the following question: which component should be charged with the mixing loss, the stator which generated the wake or the rotor through which the wake passes?

The last set of results are from the average–passage model. As stated previously, the results derived from this model of multistage turbomachinery flows should be identical to those derived from an unsteady model averaged over time. Any differences between the average–passage results and those from the unsteady rotor simulation are due to the inadequacy of the current closure models to account for the effects of the incoming unsteady flow field. Further note that the results from the

average–passage simulation would be identical to an isolated rotor simulation which incorporated the unsteady deterministic stress used in the average–passage simulation of the rotor, with inlet conditions which match the time average mass flux, the time average absolute tangential velocity, the time average radial velocity and the time averaged absolute total temperature of the unsteady simulation.

Figure 5 shows plots of the product of velocity field and density, as well as the absolute total pressure and pressure field from the rotor average–passage simulation at an axial plane corresponding to the inlet plane in the rotor unsteady simulation. Also shown in these plots are the results obtained from the rotor unsteady simulation. The agreement between the two sets of results is very good. It indicates that the unsteady flow entering the rotor is being accounted for by the existing closure models. Furthermore, one should note that the average–passage flow model gives a reasonable estimate not only of the time–averaged flow conditions to the rotor but also of the time–averaged axial impulse and the momentum flux in both the radial and tangential directions. Thus the average–passage flow model provides a correct representation of the time–averaged flow field to the rotor.

Figure 6 shows plots of the radial distribution of the mass–averaged absolute total temperature and pressure at the exit plane of the rotor as well as the predicted rotor efficiency. For comparison purposes the corresponding results derived from the unsteady rotor simulation are also shown. The agreement between the two simulations is not as good as that shown in Figure 5. The total temperature from the average–passage simulation outboard of forty percent of span is over–predicted, implying more energy is being added to the flow stream relative to that deduced from the unsteady simulation. It should be noted that both the isolated blade row simulation and the mixing plane simulation over–predicted the total temperature rise over the entire span. The average–passage total pressure plot reflects the added energy addition. The efficiency plots show the average–passage result to be in good agreement with the unsteady result to twenty percent of span, to be greater than the unsteady result between twenty and thirty–eight percent of span, and to be lower from there on. This behavior is believed to be tied to the mixing of the stator wakes as they pass through the rotor and is associated with the modeling of the wake rectification and recovery process. In general, the results from the average–passage model are in reasonable agreement with the results from the unsteady simulation. The average–passage results also suggest that accounting for the unsteady flow within the rotor passage by means of the current closure models yields results which are in far better agreement with the results from the unsteady simulation as compared to that obtained using the mixing plane model. However, as mentioned previously, there is also a clear need to further improve the closure models.

WAKE RECTIFICATION

In examining data taken downstream of a high–speed fan stage, Kerrebrock and Mikolajczak (1970) noted a circumferential nonuniformity in the total temperature field. Based on a kinematic model they were able to show that this non–uniformity was the result of the rotor wake fluid piling up on the stator pressure surface. They argued that because of the difference between the velocity of a wake fluid particle and that of a fluid particle in the free stream; a drift velocity exists which causes the wake fluid to migrate towards the pressure surface of the downstream blade. Upon impact, the component of the drift velocity normal to the blade pressure surface is lost, causing the path of a wake particle to become tangent to the pressure surface. The total temperature of a wake particle is assumed to remain constant during this process, which results in the formation of a circumferential gradient in the time–averaged total temperature at the pressure surface. For the case of a rotor, its time–averaged flow field will have a circumferential gradient in rothalpy at the pressure surface caused by the rectification of the upstream stator wake.

The results from the unsteady rotor simulation showed that, in addition to the kinematic process described by Kerrebrock and Mikolajczak (1970), there is another process by which wake rectification may occur. The process is dynamic and is the result of the interaction between the wake and the unsteady pressure field generated as the wake encounters the leading edge of a blade. For the case of a stator wake passing through a rotor, the flow physics associated with this process can be explained by referring to the inviscid nonconducting form of the equation for the rothalpy of a fluid particle. The mathematical form of this equation is

$$DI/Dt = (1/\rho)\ \partial p/\partial t \qquad (1)$$

where I is the rothalpy of a fluid particle, D/Dt is the time rate of change following a fluid particle, ρ is the density, p is the pressure, and $\partial/\partial t$ is the local time rate of change. As the wake encounters the leading edge of the rotor, the component of the wake velocity normal to the rotor surface causes the pressure field to undergo a change in time and space. According to Equation (1), the change of pressure with time will cause a change in the rothalpy of a fluid particle. The phasing in time between the rothalpy of a wake fluid particle and the unsteady pressure will cause the time–averaged rothalpy field to become spatially non–uniform. This process, as well as that described by Kerrebrock and Mikolajczak (1970), is accounted for in the average–passage model through a term which is equal to the divergence of the temporal correlation between the unsteady rothalpy and the unsteady velocity field.

The new scenario for wake rectification is illustrated by means of a series of plots which show the instantaneous contours of entropy and rothalpy as derived from the unsteady simulation of the rotor. Shown in figures 7 and 8 are five contour plots of the instantaneous entropy and rothalpy on a blade to blade surface of revolution approximately twenty percent from the hub. The time increments are equally spaced over a cycle of the wake passing period. From these plots we see that the entropy is convected towards the pressure surface of the rotor as described by Kerrebrock and Mikolajczak (1970). In addition, note that from the inlet plane to near mid–chord, the wakes are distinct and the entropy contours associated with the wakes are maintained as the wakes move down the inlet plane. Between the inlet plane of the

computational domain and the inlet plane to the rotor and perhaps as far downstream as the quarter–chord plane the unsteady flow features associated with the wake are primarily the result of inviscid flow processes. These inviscid flow features are associated with the new rectification process and are adequately resolved by the chosen numerical grid.

Figure 8 shows the rothalpy associated with the wakes. Forward of quarter chord, one observes a clear periodic change with time of the rothalpy contours associated with the wakes as they move down the inlet plane. As stated previously, the corresponding wake entropy contours are not changing with time. This change with time of the wake rothalpy contours is brought about by the unsteady pressure field as discussed above. This unsteady interaction between the pressure field and the wake leads to the rectified or time–averaged rothalpy field shown as the sixth contour plot in Figure 8. In their experimental study of rotor stator aerodynamic interactions, Hathaway et al. (1987) observed many of the features seen in these figures.

The rectification process being described is nearly isentropic, hence associated with the increase in rothalpy is a corresponding increase in the rotary total pressure. It may be possible to control and harness this increase in the rotary total pressure to enhance the performance of a rotor. One may also expect to observe a similar rectification process within stator passages which may also be controllable and lead to an increase in stator performance. These issues are beyond the scope of the current research but hopefully will be addressed in a future publication.

SUMMARY AND CONCLUSION

In this work we have conducted a series of numerical simulations to assess the need for introducing models of the effect of the unsteady deterministic flow field into simulations of the time–averaged flow field associated with a blade row embedded in a multistage machine. The first study examined the impact of this unsteady flow field on the flow across a rotor located downstream of a stator. From this numerical investigation, it was concluded that a major difference exists between the performance of the rotor operating in isolation and the same rotor operating downstream of the stator at the same time–averaged inlet flow conditions. Furthermore, it was shown that the use of a mixing plane located between the trailing edge of the stator and the leading edge of the rotor to wash out the time varying flow exiting the stator yielded results which were in better agreement with the results derived from the unsteady rotor simulation than those obtained by completely ignoring the existence of the unsteady flow state. Finally, the rotor results obtained from the average–passage model were presented. The results from the average–passage model are equivalent to those that would be obtained from an isolated rotor simulation which incorporated the deterministic stress field of the average–passage rotor simulation, with inlet conditions deduced from the average–passage simulation of the stator. The results from the average–passage simulation of the rotor were found to be in far better agreement with those from the unsteady simulation as compared to the results from the mixing plane model, especially at the inlet to the rotor. However, there is still need for further improvements in the closure models to more accurately portray the unsteady intra–blade row flow processes.

Finally, a new scenario was found leading to wake rectification. It was shown that the unsteady flow field generated as the wake created by an upstream stator blade convects past the leading edge of the downstream rotor can lead to a rectification of the rothalpy field. This unsteady process is dynamic, as opposed to the kinematic process identified by Kerrebrock and Mikolajczak (1970). The resulting rectified rothalpy field produces a rectified rotary total pressure field which may be harnessed to enhance rotor performance. It is speculated that a similar rectification process may occur within stators. Further investigation of the observed rectification process is warranted.

REFERENCES

Adamczyk, J. J., 1984, "Model Equation for Simulating Flows in Multistage Turbomachinery," ASME 85–GT–226.

Adamczyk, J. J., Celestina, M. L., Beach, T. A., Barnett M., 1990, "Simulation of Three Dimensional Viscous Flow Within a Multistage Turbine," ASME J. of Turbomachinery, Vol. 112, No. 3, July 1990, pp. 370–376.

Atkins, G. G., Jr., and Smith, L. H., Jr., 1982, "Spanwise Mixing in Axial–Flow Turbomachines," ASME J. Eng. Power, Vol. 104, No. 1, pp. 97–110.

Baldwin, B. S., and Lomax, H., 1978, "Thin Layer Approximation and Algebraic Model for Separated Turbulent Flows," AIAA 78–257.

Butler, T. L., Sharma, O. P., Joslyn, H. D., and Dring, R. P., 1989, "Redistribution of an Inlet Temperature Distortion in an Axial Flow Turbine Stage," AIAA J. of Propulsion and Power, Vol. 5.

Chen, J. P., Celestina, M. L., and Adamczyk, J. J., 1993, "A New Procedure For Simulating Unsteady Flows Through Turbomachinery Blade Passages," Submitted for presentation to the ASME 94 Gas Turbine Conference.

Dawes, W. N, 1992, "Toward Improved Throughflow Capability: The Use of Three–Dimensional Viscous Flow Solvers in a Multistage Environment," ASME J. of Turbomachinery, Vol. 114, pp. 8–17.

Dring, R. P., and Spear, D. A., 1991, "The Effect of Wake Mixing on Compressor Aerodynamics," ASME J. of Turbomachinery, Vol. 113, No. 4.

Hathaway, M. D., Suder, K. L., Okiishi, T. H., Strazisar, A. J., and Adamczyk J. J., 1987, "Measurements of the Unsteady Flow Field Within the Stator Row of a Transonic Axial–Flow Fan II," ASME 87–GT–227.

Kerrebrock, J. L., and Mikolajczak, A. A., 1970, "Intra–Stator Transport of Rotor Wakes and Its Effect on Compressor Performance," ASME J. Eng. Power, 92A, pp. 359–368.

Stewart, W. L., 1959, "Analysis of Two–Dimensional Flow Loss Characteristics Downstream of Turbomachine Blade Rows in Terms of Basic Boundary Layer Characteristics," NACA TN 3515.

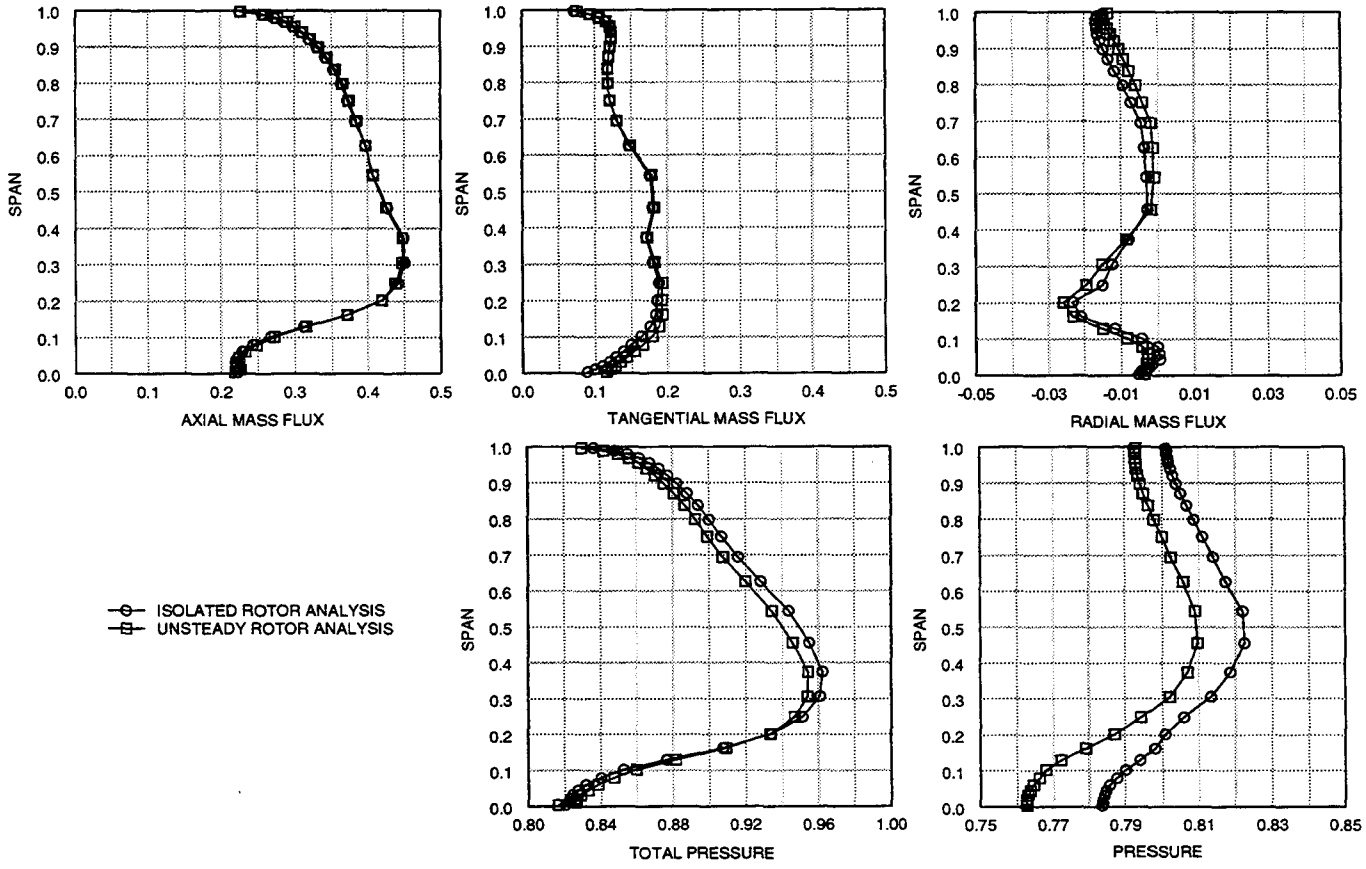

FIGURE 1. INLET FLOW CONDITIONS TO ISOLATED ROTOR ANALYSIS VS TIME AVERAGE INLET FLOW CONDITIONS DERIVED FROM UNSTEADY ROTOR ANALYSIS.

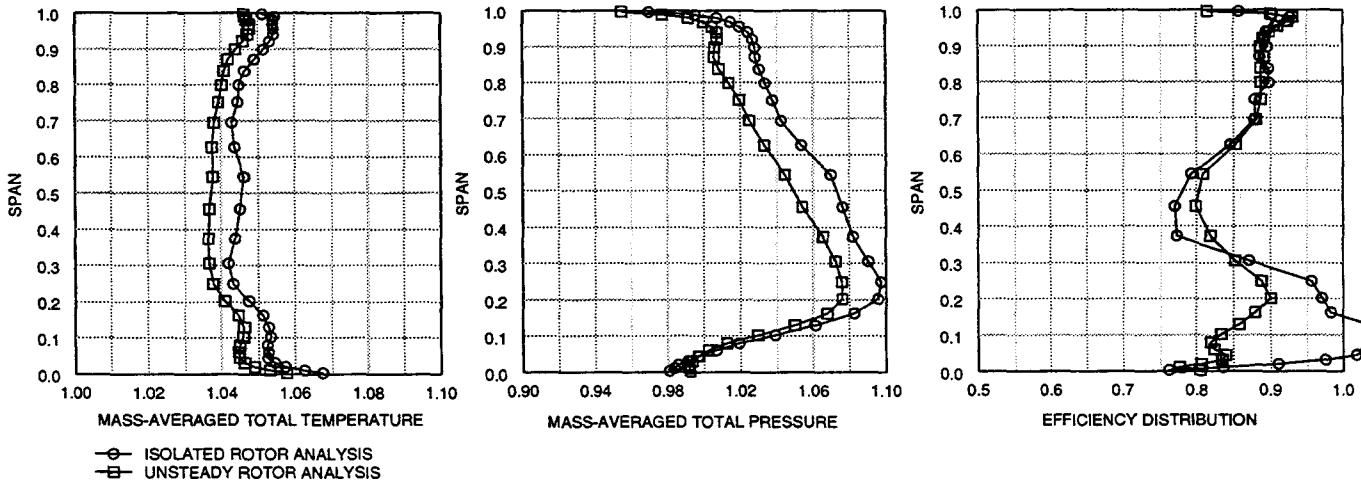

FIGURE 2. EXIT FLOW CONDITIONS DERIVED FROM ISOLATED ROTOR VS TIME AVERAGE EXIT FLOW CONDITIONS DERIVED FROM UNSTEADY ROTOR ANALYSIS.

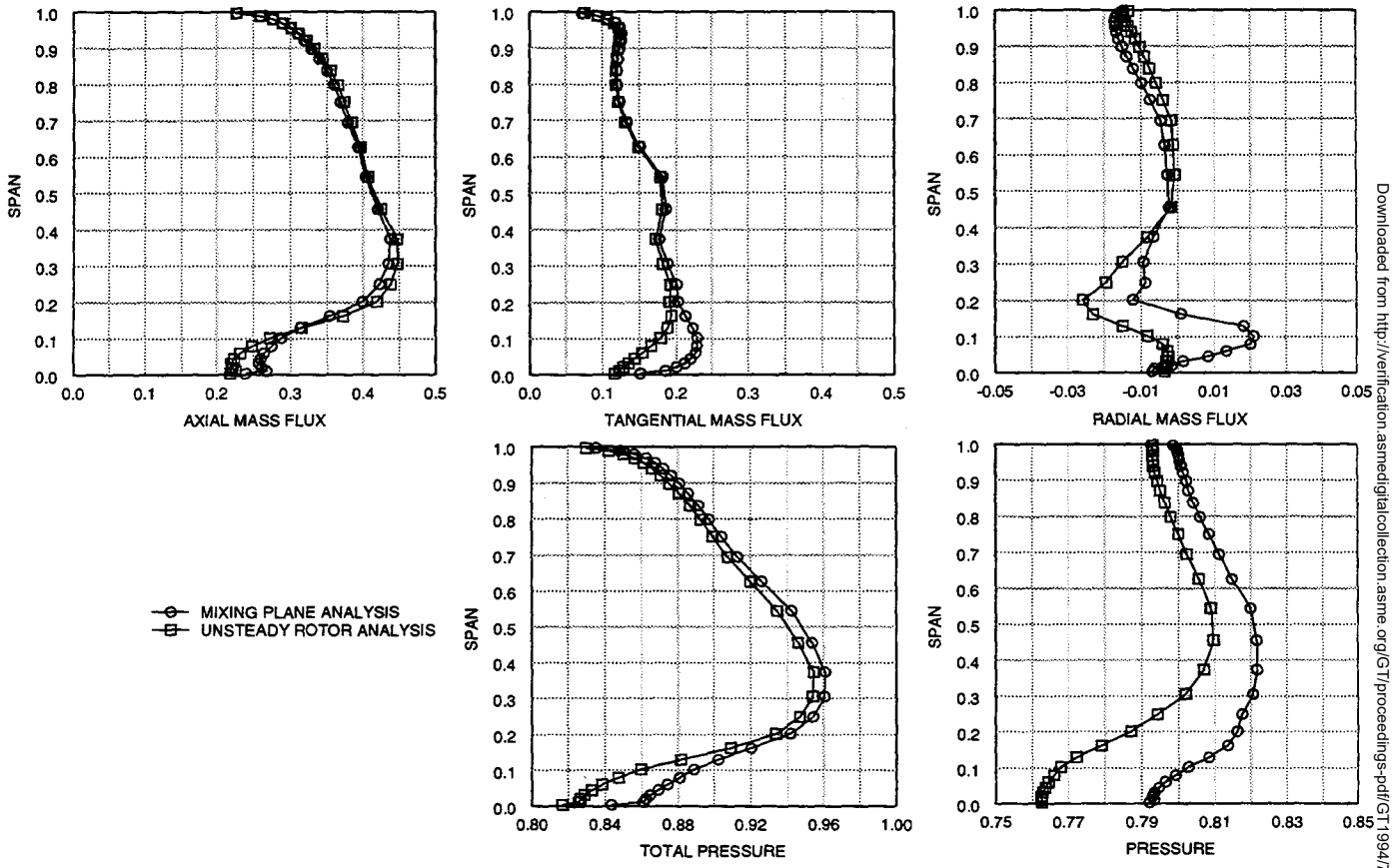

FIGURE 3. INLET FLOW CONDITIONS DERIVED FROM MIXING PLANE ANALYSIS VS TIME AVERAGE INLET FLOW CONDITIONS DERIVED FROM UNSTEADY ROTOR ANALYSIS.

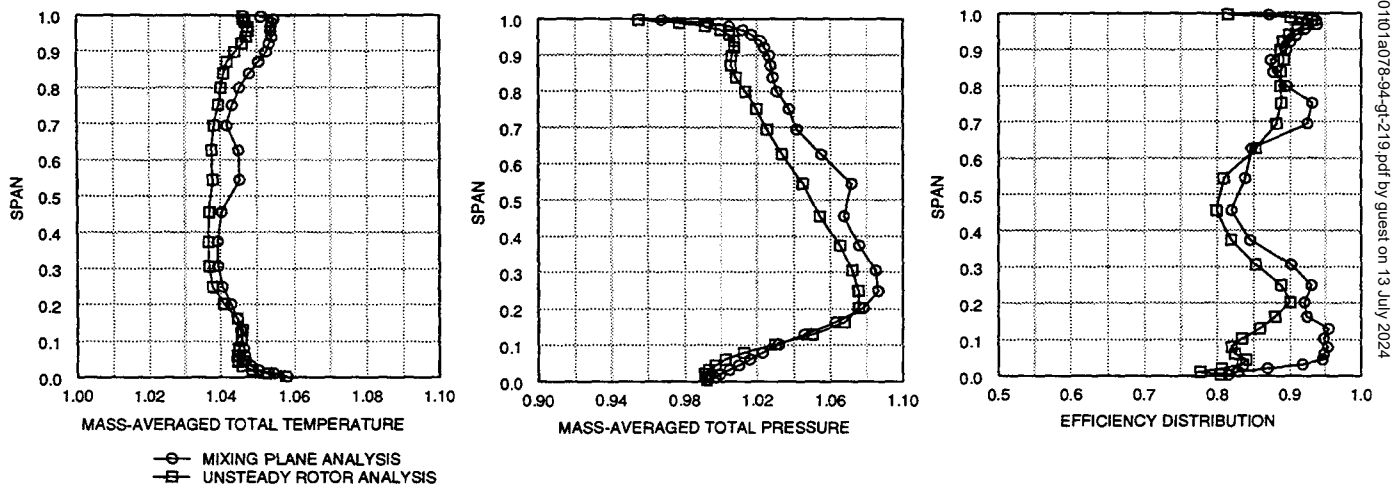

FIGURE 4. EXIT FLOW CONDITIONS DERIVED FROM MIXING PLANE ANALYSIS VS TIME AVERAGE EXIT FLOW CONDITIONS DERIVED FROM UNSTEADY ROTOR ANALYSIS.

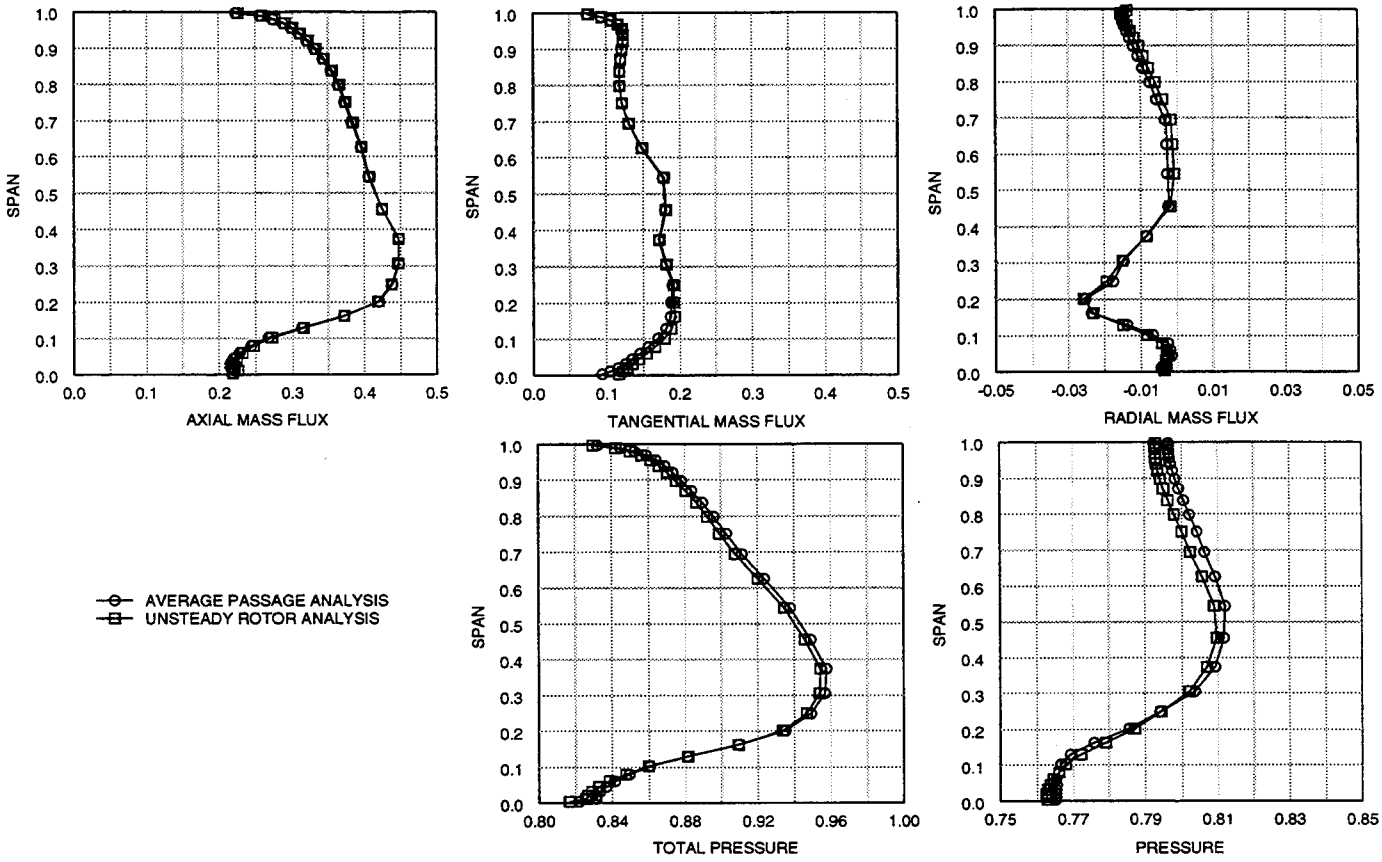

FIGURE 5. INLET FLOW CONDITIONS DERIVED FROM AVERAGE-PASSAGE ANALYSIS VS TIME AVERAGE INLET FLOW CONDITIONS DERIVED FROM UNSTEADY ROTOR ANALYSIS.

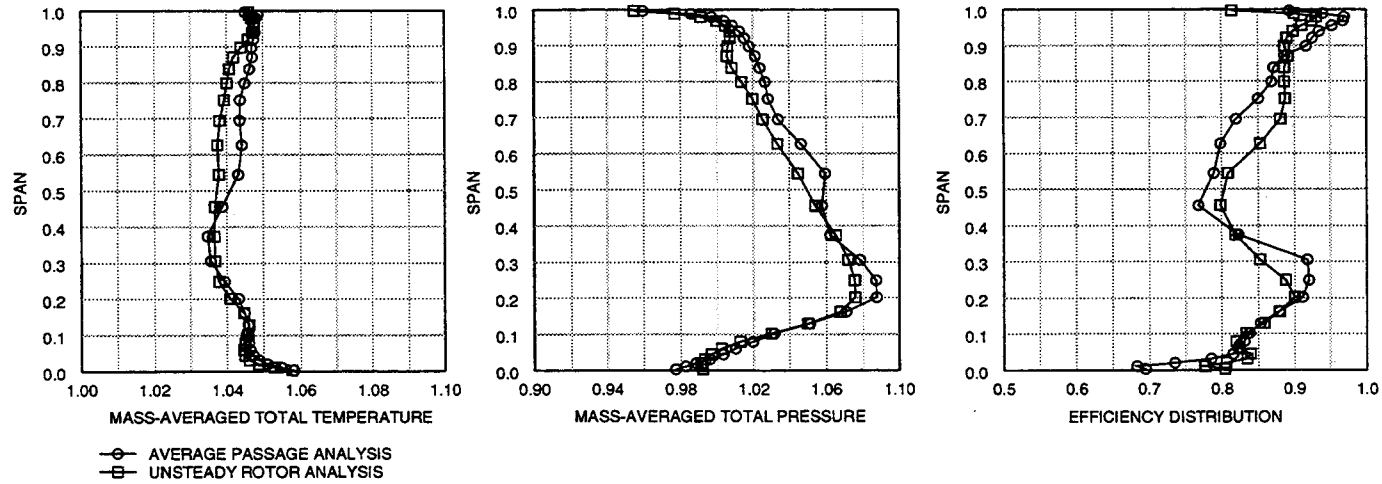

FIGURE 6. EXIT FLOW CONDITIONS DERIVED FROM AVERAGE-PASSAGE ANALYSIS VS TIME AVERAGE EXIT FLOW CONDITIONS DERIVED FROM UNSTEADY ROTOR ANALYSIS.

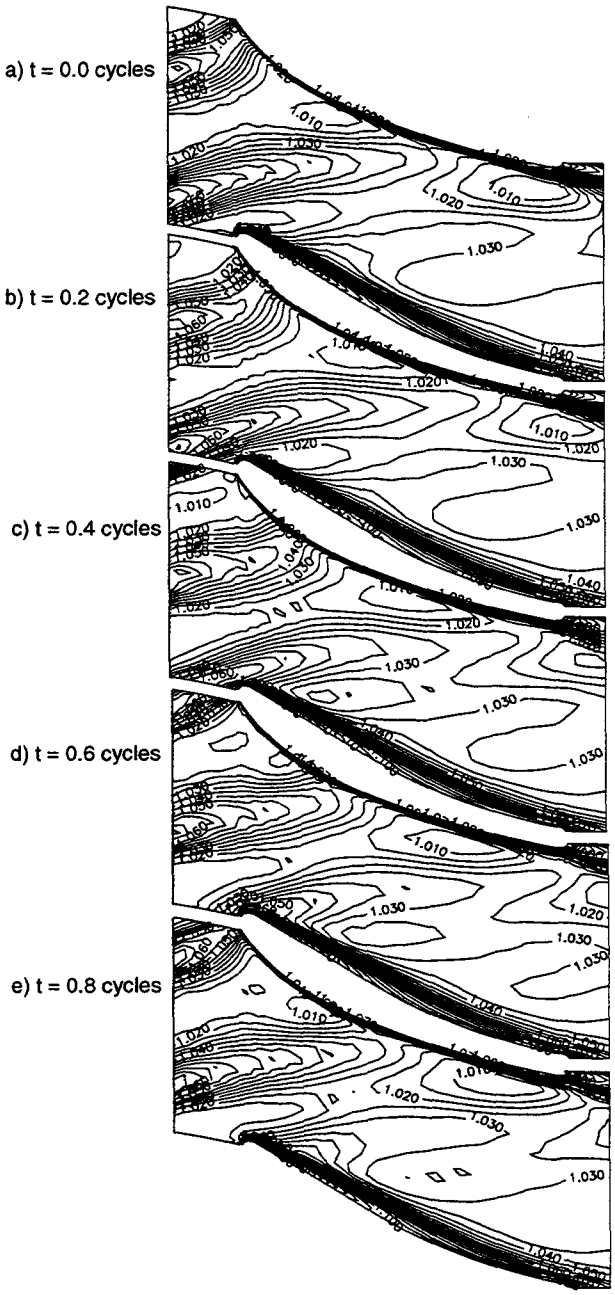

FIGURE 7. INSTANTANEOUS CONTOURS OF ENTROPY.

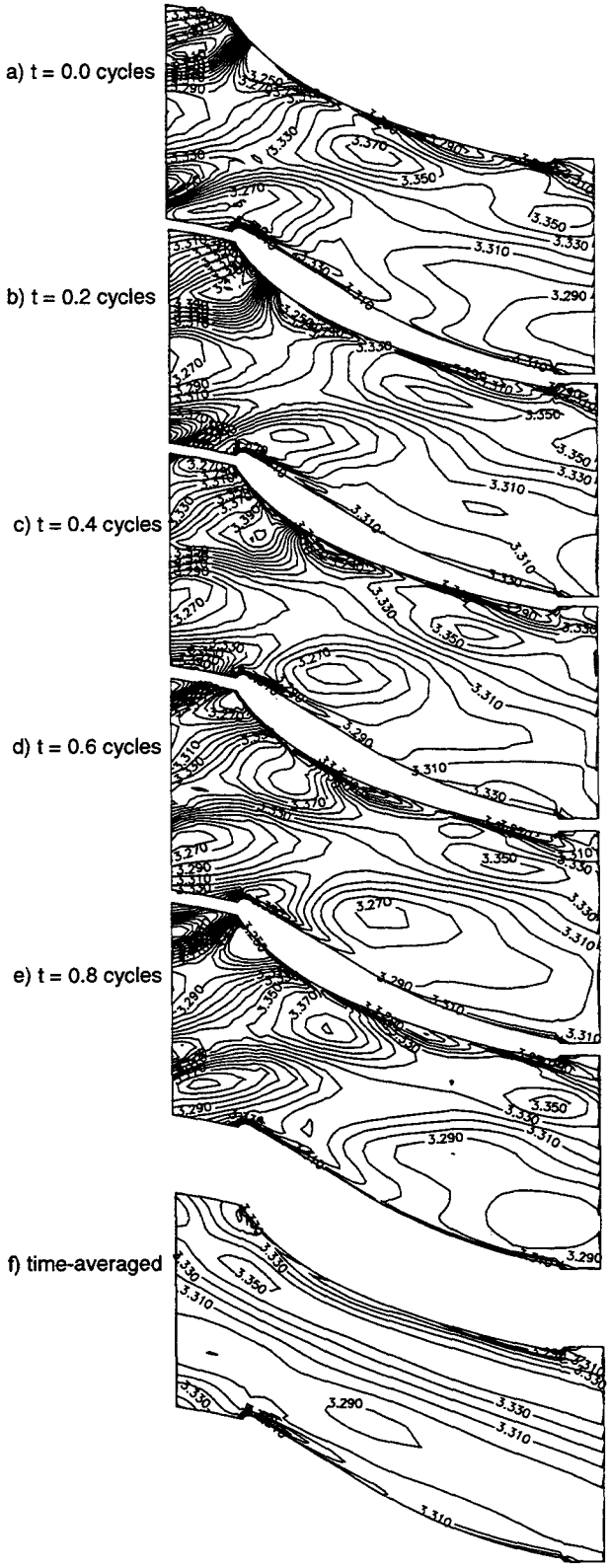

FIGURE 8. CONTOURS OF ROTHALPY.